ELSEVIER

Physica C 290 (1997) 281–290

PHYSICA C

Magnetic ac loss in multi-filamentary Bi-2223/Ag tapes

M.P. Oomen [a,*], J. Rieger [a], M. Leghissa [a], H.H.J. ten Kate [b]

[a] *Siemens AG, Corporate Technology, Erlangen, Germany*
[b] *Low Temperature Division, University of Twente, Enschede, The Netherlands*

Received 2 May 1997; revised 25 July 1997; accepted 26 July 1997

Abstract

The ac loss in high-T_c superconducting tapes with twisted and non-twisted filaments has been studied by a magnetic method. A brief overview of the theoretical background and the experimental set-up is presented. Measurements were made at 77 K in a magnetic field of 50 Hz frequency and 0.001–0.7 T amplitude. Application of dc transport current made it possible to distinguish between the loss components, arising from intra-grain and from filament currents. The magnitude of the filament loss component indicates that the filaments are fully coupled, which agrees with theory. In other measurements, the orientation of the external field with respect to the tape was varied. Knowledge of the ac loss in parallel and in perpendicular field is sufficient to predict the ac loss for any intermediate orientations of the field. © 1997 Elsevier Science B.V.

PACS: 74.25 Ha; 74.60 w
Keywords: ac loss; Magnetisation; Grain boundaries

1. Introduction

Multi-filamentary high-T_c superconducting tapes are developed for use in future power engineering applications, e.g. cables [1], transformers [2] and motors [3], which are cooled with liquid nitrogen. The cooling requirements, as well as the economic feasibility of such devices are partly determined by the energy dissipation which occurs when the tapes are subjected to a varying magnetic field. In the applications, this magnetic field is generally stronger than the self-field caused by the current in a single tape. The energy dissipated in the tapes is usually called ac loss. It is due to hysteretic screening currents in the superconducting filaments, to coupling currents between the filaments and to eddy currents in the normal-conducting sheath [4]. The loss is influenced by the geometry of the tape and its filaments, by the properties of the superconductor and of the matrix material, by the transport current in the tape (dc or ac) and by the amplitude, frequency and orientation of the external magnetic field. Theoretical predictions can be made for each of the above-mentioned loss components individually when the tape and material properties are known [4–8]. However, the total energy dissipation is determined by a complicated interaction between the loss components and therefore high-quality measurements are still essential to estimate the ac loss which will occur in the mentioned applications.

The methods for measuring ac loss can be divided into three categories. Electrical (or transport) meth-

* Corresponding author. Tel.: +49 91317 34889; fax: +49 91317 33323; e-mail: martino.leghissa@erls.siemns.de

PII S0921-4534(97)01672-9

ods [7,9] use voltage taps soldered onto the conductor, to determine the energy dissipation due to the self-field of a varying transport current: this energy is supplied by the source of the transport current. Electrical methods are adequate in situations where the effect of an external alternating field on the conductor can be ignored. With magnetic methods [7,9–11] the energy dissipation due to the various screening currents, which are induced in the conductor by an oscillating external magnetic field, is measured by means of the changes in magnetisation of the conductor. This energy is ultimately supplied by the source of the magnet current. Magnetic methods are suitable for situations in which the loss is mainly determined by the external field. Finally, calorimetric methods [12,13] are suitable to measure the total dissipated energy by means of the temperature increase which is caused in the conductor, or by the amount of cryogen that evaporates within a given time. Their accuracy is generally less than that of the other two methods and they are mainly used for large volumes or with complicated geometries where other methods would be impractical. The ac loss results reported in this paper were obtained by the magnetic method.

2. Applicable ac loss theory

2.1. Hysteresis

When a sinusoidally varying magnetic field is applied to a type-II superconductor, screening currents flowing in a surface layer along the superconductor will partially screen this field from its interior. Magnetic flux will move into and out of this surface layer, causing a hysteresis-like energy dissipation Q_h during each field cycle. The most simple description of this phenomenon is Bean's critical-state model [14] in which the screening current density is either 0 or the constant critical current density J_c of the superconductor. In that case the ac loss can be calculated for several simple geometries. The result is generally expressed in a normalized form, using the maximum field energy density [15]:

$$Q_h = \frac{2B_a^2}{\mu_0}\Gamma(\beta), \quad \beta = \frac{B_a}{B_p} \tag{1}$$

where Q_h is the dissipated energy per field cycle per m^3 of superconductor, B_a is the amplitude (half the peak-to-peak value) of the external field variation, μ_0 is the permeability of free space and Γ is a dimensionless loss function. Furthermore B_p is the penetration field: the field amplitude at which the layer of screening current fills the entire superconductor.

For an infinite superconducting slab with thickness d, parallel to the magnetic field direction, carrying no transport current, the penetration field $B_p = \mu_0 J_c d/2$ and the loss function

$$\begin{aligned} &\Gamma = \beta/3 && \text{for } \beta < 1, \\ &\Gamma = 1/\beta - 2/3\beta^2 && \text{for } \beta > 1. \end{aligned} \tag{2}$$

Similar expressions exist for superconducting cylinders parallel and perpendicular to the field. For a thin superconducting strip with the external field perpendicular to its wide side, an approximation of the ac loss for high field amplitudes is given in Ref. [7]:

$$Q_h = B_a J_c w \tag{3}$$

where w is the width of the strip. The expression given in Ref. [8] for the loss in a very thin strip in perpendicular field has the same limiting value for high field amplitudes. This ac loss is a factor w/d larger than the loss, obtained from Eqs. (1) and (2) for the same strip (modelled as an infinite slab) in high parallel fields.

The filaments of a Bi-2223 tape are flattened and they consist of weakly linked grains, oriented more or less in the plane of the filament. The grains have a much higher J_c than the filament as a whole and there is little mutual influence between the small-scale screening currents inside the grains and the larger-scale screening currents in the filament. Therefore the filaments and the grains can be treated as two independent superconducting systems [7,8], with the penetration fields $B_{p,fil}$ and $B_{p,grain}$ respectively. When the field is parallel to the wide side of the filaments, the loss in both systems can be described by Eqs. (1) and (2) and the total ac loss Q_h is the sum of the losses $Q_{h,fil}$ and $Q_{h,grain}$ in both systems. Decreasing the filament thickness d_{fil}, leads to a lower filament penetration field $B_{p,fil}$ and a lower filament hysteresis loss $Q_{h,fil}$ for field amplitudes $B_a > B_{p,fil}$. Finally, the dissipated energy per

field cycle per m^3 of tape can be calculated by multiplying the result of Eq. (1) or Eq. (3) by the volume fraction of superconducting material in the tape.

2.2. Inter-filament coupling

In multi-filament superconducting tapes, the filaments can be made very thin and this decreases the filament hysteresis loss as explained above. However, an extra ac loss Q_c is caused by coupling currents which partially screen the entire multi-filamentary core of the tape from the external field variations. In a tape sample with non-twisted filaments, these coupling currents follow the filaments on one side until they reach the end of the sample. There they cross the normal-conducting matrix and flow back along the other side in a closed loop.

For low field amplitudes B_a and field frequencies $\omega = 2\pi f$, the coupling loss Q_c can be calculated [4,6] using

$$Q_c = \frac{n\pi B_a^2 \omega\tau}{\mu_0(1+\omega^2\tau^2)} \tag{4}$$

where the shape factor n and the time constant τ depend upon the properties of the multi-filamentary core of the conductor. For instance, a thin rectangular conductor with its wide side parallel to the field has $n = 1$ and a time constant

$$\tau = \mu_0 \sigma_c L_p^2 \frac{d_c^2}{16 w_c^2} \tag{5}$$

where σ_c is the cross-conductivity of the core, L_p is the filament twist pitch and d_c and w_c are the core thickness and width, respectively. As long as $\omega\tau < 1$, the coupling loss Q_c given by Eq. (4) can be made smaller by decreasing τ, which can be done by decreasing σ_c or (more effectively) by decreasing the twist pitch L_p.

This model assumes that the coupling currents flow without resistance in the outer layer of filaments, which is possible only when the currents are smaller than the total critical current of these filaments. For larger B_a and larger ω, more and more filaments will be saturated with their critical current. Finally, the filaments are fully coupled: the entire core of the conductor behaves like one large filament [16]. The onset of full coupling can be predicted by comparing the conductor's critical current to the total coupling current in the outer filaments, which can be calculated from the electric field distributions given in Ref. [4] for several geometries. For parallel field, the occurrence of full coupling can also be predicted with a simple model [15]: two superconducting slabs (the filaments) with thickness d_{fil} are separated by a normal-conducting layer with conductivity σ. The slabs are saturated with their critical current (i.e. they are fully coupled) if the sample is longer than the critical coupling length L_c:

$$L_c = 4\sqrt{\frac{d_{fil} J_c}{2\sigma\omega B_a}}\,. \tag{6}$$

This coupling length must be compared to the sample length for tapes with non-twisted filaments, or to one-half the twist pitch for twisted-filament tapes. For a given field amplitude B_a and frequency ω, filament twist decreases the coupling currents only if the twist pitch L_p is made smaller than $2L_c$.

When there is full coupling, the loss Q_c is no longer determined by the cross-conductivity of the core, as in Eqs. (4) and (5). Instead, Q_c is limited by the critical current in the filaments. In this case the coupling loss can be described by the Bean critical-state model, applied to the entire tape core which behaves like a single large filament. The loss Q_c can then be calculated with Eqs. (1) and (2) or Eq. (3) if the core thickness, core width and core-average critical current density are used instead of the filament or grain properties.

2.3. Sheath eddy currents

Even if the tape would contain no superconductor, a varying magnetic field would induce eddy currents in the normal-conducting matrix and sheath material. These eddy currents cause an ohmic energy dissipation Q_e. If the superconductor does not influence these currents, and if the matrix and sheath materials have the same conductivity σ, the eddy current loss for a rectangular conductor can be calculated [17] using

$$Q_e = \pi\omega B_a^2 \sigma \frac{w_\perp^2}{12} \tag{7}$$

where $w_\perp$ is the width of the conductor in the direction perpendicular to the external field. This is the tape width if the field is oriented perpendicular to the wide side of the tape, or the tape thickness if the field is oriented parallel to this side.

The eddy current loss Q_e is generally small in comparison with the other loss components. However, at high field amplitudes B_a the hysteresis loss Q_h and full-coupling loss Q_c are both proportional to B_a, while Q_e is proportional to ωB_a^2. Therefore Q_e can become important for high B_a and high ω. Finally, at high frequency the eddy loss is smaller than the value from Eq. (7) due to the skin effect.

2.4. The total ac loss

The total ac loss induced in a superconductor tape by a varying external magnetic field may be estimated by summing the loss contributions discussed in the previous sections:

$$Q_{total} = Q_h + Q_c + Q_e = Q_{h,fil} + Q_{h,grain} + Q_c + Q_e \quad (8)$$

where Q_{total} is the dissipated energy per field cycle per m^3 of tape. However, if Q_{total} would be calculated using Eqs. (1)–(8) (for an external field parallel to the tape plane), the following effects would not be taken into account:

- Q_h and Q_c are lower due to shielding of the tape core by the sheath eddy currents.
- Q_h is lower due to shielding of the inner filaments by the coupling currents.
- $Q_{h,fil}$ is lower when part of the available space in the filaments is filled by coupling currents. For full coupling $Q_{h,fil}$ is expected to disappear.
- Q_c is unknown in the region between limited coupling (Eqs. (4) and (5)) and full coupling.
- Q_c may be much higher if there are superconducting intergrowths between the filaments.
- J_c in the filaments and in the grains is decreased by the local magnetic field.
- Flux creep and flux flow cause a non-linear V–I curve instead of a well-defined J_c. This can have several effects, e.g. Q_h can be frequency-dependent [7].
- Transport current can affect all three loss components.

For most of these interaction effects between the loss components, advanced theoretical models can be found in the literature, e.g. Refs. [4,7,15].

3. The experimental method

A conventional method for measuring the ac loss induced in a sample by an oscillation in the external field $\boldsymbol{B}$ is by detecting the changes in magnetic moment $\boldsymbol{m}$ of the sample [7,8,10,11,15]. The dissipated energy in the entire sample volume V_{sample} can then be calculated with

$$Q_{total}V_{sample} = \oint_{field\,cycle} \boldsymbol{B}\cdot d\boldsymbol{m} = \int_T \boldsymbol{B}\cdot\frac{d\boldsymbol{m}}{dt}dt = \int_T Bm'_{\parallel}\,dt \quad (9)$$

where t is time and T is the duration of a field cycle. During this period it is necessary to measure the field strength B and the rate of change $m'_{\parallel}$ of the component of $\boldsymbol{m}$ parallel to $\boldsymbol{B}$. This rate of change is detected as a voltage over a pick-up coil around the sample, whose windings are oriented in a plane perpendicular to $\boldsymbol{B}$ in order to make sure that only the parallel component of $\boldsymbol{m}$ is detected. A much larger signal is induced in this pick-up coil by the external field variation B'. This signal is compensated for by a second similar coil some distance away from the sample, which is connected in anti-series to the pick-up coil. The combined signal is

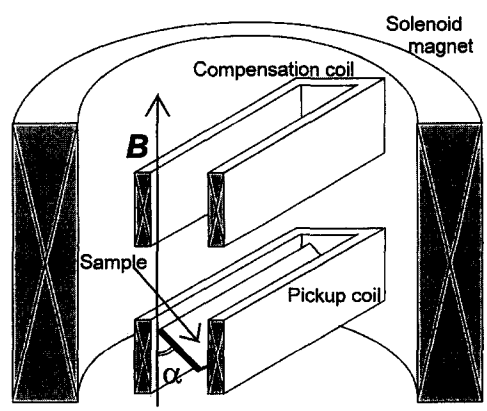

Fig. 1. Insert for examining short tape samples at any field angle α.

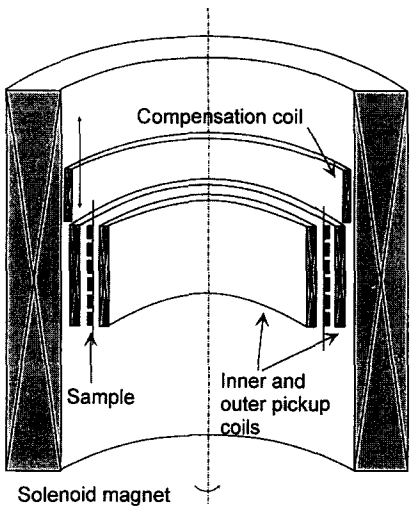

Fig. 2. Insert for examining long tape samples with transport current in parallel field.

multiplied by the magnetic field strength B (which is measured via the magnet current) and integrated over an integer number of field cycles to give the ac loss.

Our measurement set-up is based on a solenoid magnet, which can generate a magnetic field strength of 0–0.7 T. This magnet is part of an LC resonant circuit, so that field frequencies of 50–500 Hz (the power frequency range) are possible. The magnet and its contents are cooled to 77 K by a bath of liquid nitrogen. Two inserts have been constructed for this magnet. One of them (see Fig. 1) is suitable for examining straight tape samples of up to 95 mm long. The samples are placed right across the magnet bore, with their longitudinal direction perpendicular to the field. The pick-up and compensation coils are rectangular and the angle α between the field direction and the wide side of the tapes can be varied between 0° and 90°.

In the other insert (see Fig. 2), tape samples of up to 2 m long can be wound on a sample holder (radius 37 mm) which is placed between an inner and an outer pick-up coil. The signals induced in both these pick-up coils by the magnetic moment change $m'_{\|}$ add up, while the signals induced by B' cancel out. Any remaining signal induced by B' is removed by a small movable compensation coil. In this insert the tapes can only be oriented with their wide side parallel to the field ($\alpha = 0°$). A constant transport current can be supplied to the sample and the critical current can be measured by means of voltage taps (not shown in Fig. 2).

4. Results and discussion

4.1. Properties of the examined tapes

The ac loss results reported in this paper were all obtained with 55-filament Bi2223/Ag tapes, produced with the powder-in-tube process. Details of the tape preparation are described in Ref. [1]. Some properties of the examined tapes are listed in Table 1.

4.2. Effect of filament twist on the ac loss

The ac loss measured in Tape A with twisted and non-twisted filaments is presented here in the form of the dimensionless loss function $\Gamma = \mu_0 Q_{\text{total}}/2B_a^2$ defined in Eq. (1). Here Q_{total} is the dissipated energy per field cycle per m^3 of tape material. For external fields with a frequency of 50 Hz, parallel

Table 1
Properties of the tapes investigated in this paper

Type	Tape A non-twisted	Tape A twisted	Tape B
Width (mm)	3.9	3.5	3.8
Thickness (mm)	0.25	0.25	0.25
Matrix material	Ag	Ag	Ag
Sheath material	Ag/0.5% Mg	Ag/0.5% Mg	Ag
Twist pitch	–	20	–
Bi-2223 fraction	25%	25%	25%
Critical current (A) at 77 K	42	36	40

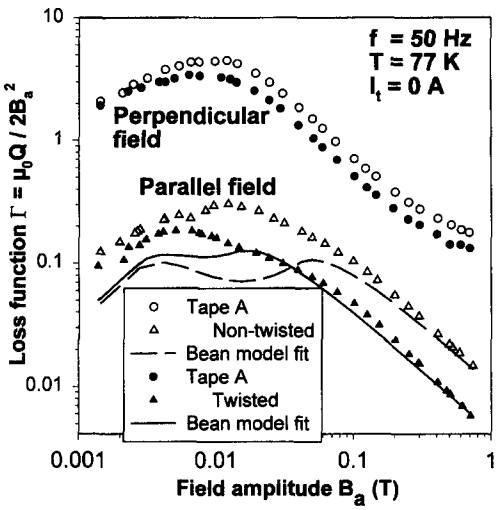

Fig. 3. ac loss measured in Tape A with twisted and non-twisted filaments.

and perpendicular to the wide side of the tapes, Γ has been logarithmically plotted against the field amplitude B_a in Fig. 3.

For low field amplitudes B_a the measured loss functions increase with B_a, while for high B_a they decrease in proportion to $1/B_a$. This is in accordance with the parallel-field hysteresis loss function as in Eq. (2), indicating that the ac loss is dominated by hysteresis. For high B_a the loss in perpendicular field is larger than that in parallel field by about a factor 10, which is close to the aspect ratio w/d of the tapes. This agrees with the prediction for hysteresis loss in a thin strip, made in Section 2.1. Finally, the ac loss in the twisted-filament tape is lower than the loss in the non-twisted tape by a factor of 1.5–2, which is more than their difference in critical current (see Table 1). This cannot be understood if the loss is caused only by hysteresis within the filaments and the grains: in that case filament twist would have no effect at all.

The losses measured for parallel field have been fitted with the sum of two loss functions according to the Bean critical-state model: one for the filaments and one for the grains. Both loss functions have the form of Eq. (2), but they may have different penetration fields B_p. These fields $B_{p,fil}$ and $B_{p,grain}$ are the only two parameters of the fit, as the volume fraction of superconductor in the tapes is known. Both of the fitted loss function in Fig. 3 have $B_{p,fil} = 0.003$ T. The loss function for the twisted tape (solid line) has $B_{p,grain} = 0.015$ T, while the one for the non-twisted tape (dashed line) has $B_{p,grain} = 0.040$ T. However, the fitted loss functions do not describe the measurement results for low field amplitudes B_a. These deviations at low B_a could be decreased by making $B_{p,grain}$ smaller, but this would result in deviations at high B_a. Furthermore the deviations vary with B_a, so they are not caused by coupling current loss as described by Eq. (4) or by eddy current loss as described by Eq. (7): these would result in a loss function Γ independent of B_a. This indicates that the ac loss model based on hysteresis in separate filaments does not apply here (see also Section 4.4). Comparison with other ac loss models is difficult here, due to the unknown relative importance of the various loss contributions.

4.3. Effect of a dc transport current

When a dc transport current is supplied to a Bi-2223/Ag tape, the current is shared between the superconducting filaments and the normal-conducting matrix, due to imperfections of the superconductor. From the voltage measured over a certain length of tape, the current components flowing in the matrix and in the filaments can be calculated. A typical

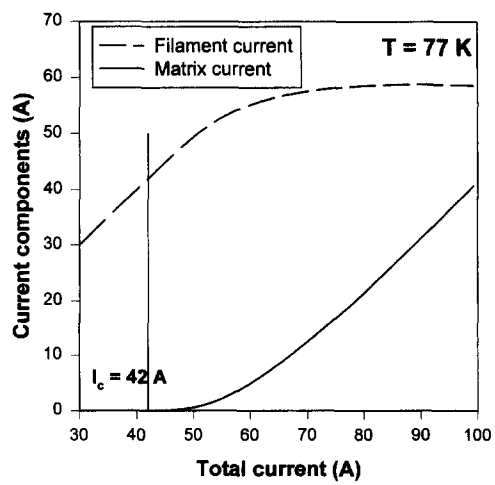

Fig. 4. Current sharing between superconductor and matrix in non-twisted Tape A.

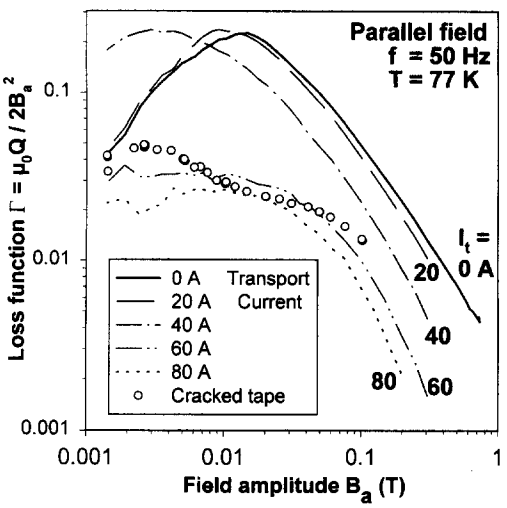

Fig. 5. ac loss measured in Tape B with various dc transport currents.

result obtained with the non-twisted Tape A is displayed in Fig. 4, where both current components are plotted against the total transport current I_t. For increasing I_t the current in the filaments increases up to $I_t = 60$ A and remains practically constant for $I_t > 60$ A. This can be understood by considering that the filaments are inhomogeneous: over large parts of their length they can carry a total current which is larger by about a factor 1.5 than the critical current $I_c = 42$ A, obtained with the 10^{-4} V/m criterion.

In Tape B with non-twisted filaments, the ac loss was measured while dc transport currents of up to 80 A ($= 2 * I_c$) were supplied to the tape. The resulting loss functions Γ, measured with the field parallel to the wide side of the tape, have been logarithmically plotted against the field amplitude B_a in Fig. 5 (lines). (The electrical energy supplied to the tape by the transport current source, which also depends on B_a, was not measured in these experiments.) Fig. 5 also contains the loss function Γ measured in the same tape after it has been bent over a radius of about 2 mm (dots). This bending has caused many cracks in the filaments, so that superconducting currents can only flow over short distances along the tape.

A transport current $I_t = 40$ A has a clear influence on the loss function: the maximum of Γ shifts to lower field amplitudes. This can be understood by considering that the transport current occupies some space in the filaments, which could otherwise be filled with screening or coupling currents. This decreases the effective thickness d and the penetration field B_p of the system. When I_t is further increased to 60 A, the loss decreases greatly at all field amplitudes. Finally, increases in I_t beyond 60 A cause little further decrease in the loss. Comparison with the current-sharing results for a similar tape, displayed in Fig. 4, indicates that a transport current of about 60 A completely fills the filaments, suppressing all large-scale screening or coupling currents. The remaining ac loss at $I_t > 60$ A is caused by small-scale screening currents inside the superconducting grains. The grains have a much higher critical current density J_c than the filament as a whole. Therefore the intra-grain currents are practically not influenced by I_t [17]. Finally, when the tape is bent over a small radius, most of the large-scale currents in the broken filaments are suppressed [8]. Therefore the loss measured in the cracked tape (dots in Fig. 5) is close to the loss in the undamaged tape at $I_t = 60$ and 80 A (solid lines), where the large-scale currents are suppressed by I_t.

If the screening currents in the grains are not significantly influenced by the transport current I_t, the ac loss $Q_{h,grain}$ is independent of I_t. Then according to Eq. (8), $Q_{h,grain}$ (obtained from the measurements with $I_t = 60$ A and 80 A) can be subtracted from Q_{total} (measured at $I_t = 0$ A), to obtain $Q_{h,fil} + Q_c$ the ac loss caused by large-scale screening and coupling currents following the filaments. (The eddy current loss Q_e is relatively small in parallel field and can be ignored here.) The two loss components obtained in this way for Tape B have been plotted against field amplitude B_a in Fig. 6. The total ac loss in this tape is dominated by the filament loss component $Q_{h,fil} + Q_c$. The loss function Γ for the filaments (open dots) behaves according to Eq. (2): it is proportional to B_a at low field, proportional to $1/B_a$ at high field and it has a clear maximum at $B_a = 0.015$ T. However, the loss function for the grains (solid triangles) does not have such a clear maximum. The grains seem to have penetration fields $B_{p,grain}$ ranging from 0.001 to 0.02 T. This is probably due to stacks or clusters of grains, which can have a wide distribution of sizes and coupling strengths [8].

4.4. Full coupling of the filaments

The loss function from the Bean critical-state model for a superconducting slab parallel to the field (Eq. (2)) has been fitted to the filament loss found in Tape B (open dots in Fig. 6), accounting for the known superconductor fraction of 25% in the tape. The result (dashed line) is evidently too small to explain the entire filament loss. However, at a field amplitude $B_a = 0.001$ T, the critical coupling length L_c calculated with Eq. (6) is about 16 mm for this tape. This is much smaller than the sample length of about 1 m, indicating that the filaments are fully coupled for the entire field range used in the measurements. Then the entire tape core behaves like a single large filament and its loss function in parallel field can again be described by Eq. (2). Microscopic photographs show that the core is a flattened ellipse which fills about 50% of the tape volume. This is used to calculate a new fit function (solid line in Fig. 6), which is a much better description for the measured filament loss. The penetration field found from this fit $B_{p,core} = \mu_0 J_c d_c/2 = 0.0085$ T. This gives an effective core thickness $d_c = 161$ μm, close to the real core thickness of 175 μm obtained from the microscopic photographs. This is a strong indication that the filaments are indeed fully coupled.

The loss function Γ measured in Tape B with the field perpendicular to the wide side of the tape, has

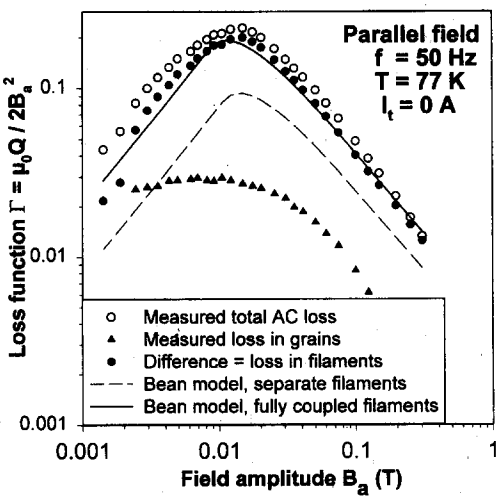

Fig. 6. ac loss in grains and filaments of Tape B.

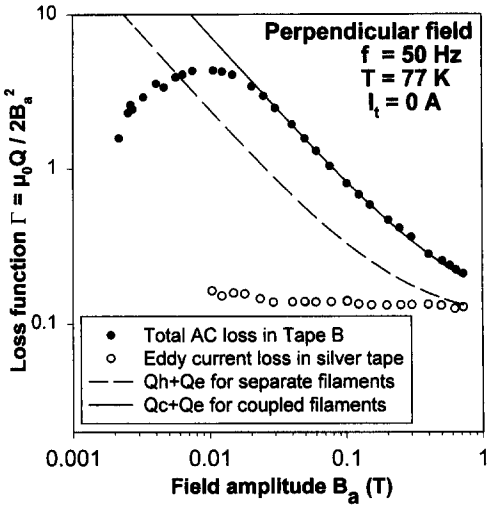

Fig. 7. ac loss in Tape B in perpendicular field.

been plotted as solid dots in Fig. 7. For high B_a this loss can be described by the high-field limit of the critical-state model for a thin superconducting strip, given in Eq. (3). However, the eddy current loss in the silver sheath cannot be ignored in this case. The eddy loss measured in a pure silver tape of 3.5×0.25 mm^2, with the field perpendicular to its wide side, has been plotted in Fig. 7 as open dots. This loss function is practically constant and it agrees with Eq. (7) if an effective tape width $w_\perp = 2.7$ mm is assumed. This $w_\perp$ is somewhat smaller than the real tape width, which is probably due to the skin effect: the skin depth at 77 K and 50 Hz is close to the tape width.

The eddy current loss found in the pure Ag tape has been multiplied by 0.75, which is the fraction of Ag in a superconducting tape. Then this loss has been added to the loss function calculated with the high-field limit for a thin strip, as given by Eq. (3). A strip width $w = 0.50$ mm was used, which corresponds to the widest filaments seen in microscopic photographs. The loss in the grains is ignored here: we expect that it is only a small fraction of the total loss for high B_a, as it is in parallel field (see Fig. 6). The calculation result, displayed as a dashed line in Fig. 7, is evidently lower than the measured loss. The solid line is the result calculated in the same way for a fully coupled tape core, where the effec-

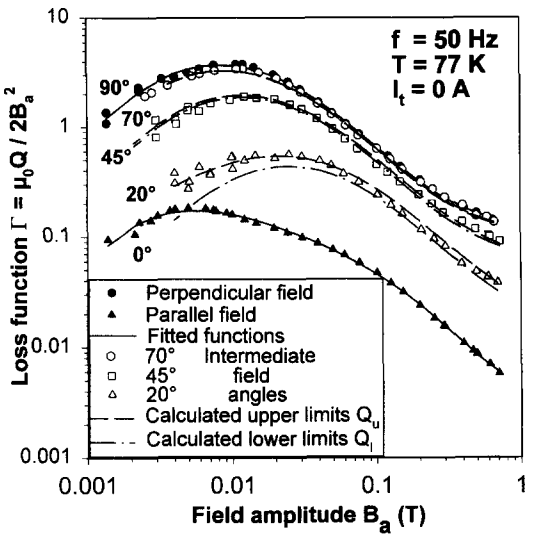

Fig. 8. ac loss in twisted-filament Tape A for various field angles.

tive core width $w_c = 2.68$ mm. It describes the measured loss very well for field amplitudes $B_a > 0.02$ T. This indicates that the filaments are also fully coupled when the field is perpendicular to the wide side of the tape.

4.5. Dependence of ac loss on the field angle

In applications like transformers and motors, the external field which causes ac loss may be oriented at any angle with respect to the tape plane. The dependence of the ac loss on the field angle α (see Fig. 1) has been measured in Tape A twisted and non-twisted. The results for the twisted-filament tape are displayed in Fig. 8, where the loss function Γ for several field angles has been logarithmically plotted as dots against the field amplitude B_a. For intermediate field angles α, the maximum in Γ lies at higher B_a than for either $\alpha = 0°$ (parallel field) or $\alpha = 90°$ (perpendicular field).

Measurement effort can be saved if the results for any α can be predicted from the losses measured in parallel and/or perpendicular field. Such a prediction can be made in the following way [18]. For any field angle α, the magnetic field $\boldsymbol{B}$ is split up in a component $\boldsymbol{B}_{\parallel}$ parallel to the tape plane and a component $\boldsymbol{B}_{\perp}$ perpendicular to it. If $\boldsymbol{B}_{\parallel}$ would be applied independently, it would cause an ac loss $Q_{\parallel}$ which is calculated here with a suitable mathematical function: the lower solid line in Fig. 8. This function has been fitted to the loss measured in parallel field (closed triangles). The same is done for the loss $Q_{\perp}$ that would be caused by the perpendicular field component $\boldsymbol{B}_{\perp}$ (upper solid line and closed dots). The losses $Q_{\parallel}$ (parallel field component) and $Q_{\perp}$ (perpendicular field component) are then added together to provide an upper limit Q_u for the loss at field angle α (dashed lines in Fig. 8). Finally, a lower limit Q_l is obtained by taking the loss $Q_{\perp}$ that would be caused by only the perpendicular field component (dash-dot lines). The calculation is straightforward:

$$\text{dashed lines: } Q_u(B_a,\alpha) = Q_{\perp}(B_{a\perp}) + Q_{\parallel}(B_{a\parallel})$$
$$= Q_{\perp}(B_a \sin\alpha) + Q_{\parallel}(B_a \cos\alpha), \quad (10)$$

$$\text{dash - dot lines: } Q_l(B_a,\alpha) = Q_{\perp}(B_{a\perp})$$
$$= Q_{\perp}(B_a \sin\alpha). \quad (11)$$

The theoretical background for this procedure is discussed in Ref. [18]; the main points are summarised here. At low field amplitudes B_a, the tape can simultaneously carry the two current patterns that would be induced by the field components $\boldsymbol{B}_{\parallel}$ and $\boldsymbol{B}_{\perp}$, if these were applied independently. These current patterns cause the losses $Q_{\parallel}$ and $Q_{\perp}$ respectively, which can be added together as in Eq. (10). At high B_a there is room in the superconducting grains and filaments for only the current pattern that would be induced by $\boldsymbol{B}_{\perp}$. Therefore only the loss $Q_{\perp}$ occurs, as in Eq. (11).

The two predicted limits Q_u and Q_l (displayed in Fig. 8 by their respective loss functions Γ) form a good approximation to the measured loss at intermediate α (open dots). They describe the shifting of the maximum in Γ towards larger field amplitudes B_a. Furthermore, for most field angles α the difference between Q_u and Q_t is relatively small. The procedure given above leads to a loss prediction which is accurate to within 10% for all examined tapes.

5. Conclusions

The ac loss in multi-filamentary Bi-2223/Ag tapes was measured for various orientations of the oscillating external field. The results can be de-

scribed by a rather simple expression in terms of the ac loss measured in parallel and perpendicular field. Measurements at these two field orientations are therefore sufficient to predict the loss in applications where the external field orientation varies.

The measurements where dc transport current and ac magnetic field were simultaneously applied to the tape made it possible to separate the ac loss components, caused by intra-grain screening currents and by large-scale currents following the filaments. The results indicate that the filaments are fully coupled: the entire core of the tape behaves like one large filament, in parallel as well as in perpendicular field. This is probably true for all similar tapes with a highly conductive silver matrix between the filaments. It explains why the measurement results cannot be quantitatively explained by a double critical-state model (for grains and filaments) if separate filaments are assumed.

Calculations of the critical coupling length indicate that the matrix resistance must be considerably increased, and the filaments tightly twisted, in order to suppress full filament coupling in Bi-2223/Ag tapes at the field frequencies and amplitudes used in these experiments. These requirements will become somewhat less stringent when the critical current of the filaments increases.

Full coupling does not explain the difference of about a factor 2 in ac loss between the examined tapes with twisted and non-twisted filaments. Further examination of twisted and non-twisted tapes is necessary in order to understand this difference.

Acknowledgements

This work has been supported by the German BMBF (contract No. 13N6481). The authors express their thanks to Dr. Ries for helpful discussions, and to H. Krauth and T. Arndt (VacuumSchmelze GmbH) and B. Roas and B. Fischer (Siemens AG), for preparing the examined samples.

References

[1] M. Leghissa, B. Fischer, B. Roas, A. Jenovelis, J. Wiezoreck, S. Kautz, H.-W. Neumüller, C. Reimann, R. Nanke, P. Müller, ASC Conference, Pittsburgh, August 25–30. 1996.
[2] M. Iwakama, K. Funaki, H. Shinohara, T. Sadohara, M. Takeo, K. Yamafuji, M. Konno, Y. Kasagawa, K. Okubo, I. Itoh, S. Nose, M. Ueyama, K. Hayashi, K. Sato, ASC Conference, Pittsburgh, August 25–30. 1996.
[3] J.P. Voccio, B.B. Gamble, C.B. Prum, H. Picard, ASC Conference, Pittsburgh, August 25–30. 1996.
[4] A.M. Campbell, Cryogenics 22 (1982) 3.
[5] W.T. Norris, J. Phys. D 3 (1970) 489.
[6] K. Kwasnitza, St. Clerc, Physica C 233 (1994) 423.
[7] St.H.-R. Clerc, PhD thesis, Swiss Federal Institute of Technology, Zurich, 1995.
[8] K.-H. Müller, C. Andrikidis, H.K. Liu, S.X. Dou, Physica C 247 (1995) 74.
[9] M. Ciszek, A.M. Campbell, S.P. Ashworth, B.A. Glowacki, Appl. Supercond. 3 (1995) 509.
[10] T.A. Buchhold, Cryogenics 9 (1963) 141.
[11] G.C. Montanari, I. Ghinello, L. Gherardi, P. Caracino, Supercond. Sci. Technol. 9 (1996) 385.
[12] E. Béghin, J. Bock, G. Duperray, D. Legat, P.E. Herrmann, Appl. Supercond. 3 (1995) 339.
[13] P. Dolez, M. Aubin, D. Willen, R. Nadi, J. Cave, Supercond. Sci. Technol. 9 (1996) 374.
[14] C.P. Bean, Phys. Rev. Lett. 8 (1962) 250.
[15] M.N. Wilson, Superconducting Magnets, Clarendon, Oxford, 1983.
[16] Y. Fukumoto, H.J. Wiesmann, M. Garber, M. Suenaga, P. Haldar, Appl. Phys. Lett. 67 (1995) 3181.
[17] M.J. Woudstra, Graduation Report, University of Twente, The Netherlands, 1995.
[18] M.P. Oomen, J. Rieger, M. Leghissa, H.H.J. ten Kate, Appl. Phys. Lett. 70 (1997) 3038.